

The fundamental limit of small antenna bandwidth: How it affects small GPR antennas

C.J.Leat, member IEEE

Abstract— **A numerical implementation of the Chu fundamental limit for small antennas was used to reveal that above typical ground materials, GPR antennas may be reduced to 65 % of the size of free space antennas before the small size seriously constrains the bandwidth or efficiency.**

I. INTRODUCTION

Observation of the dimension and centre frequency of a number of commercial GPR dipole antennas, particularly those designed for 50MHz and below, reveals that they approach the limits for small antennas if we consider them in vacuo. For example, one manufacturer provides an antenna of centre frequency 35MHz and maximum dimension 2m. This invites the question of the extent to which the presence of the ground half-space mitigates the problems of obtaining high bandwidth and efficiency for antennas of a given size and centre frequency.

In 1948 L.J.Chu [1] developed a theoretical basis to explain the observed phenomenon that electrically small antennas were narrow-band. In the process, he was also able to theoretically describe the bandwidth penalties that are incurred when small omnidirectional antennas are required to have high directivities. Chu's approach was to conceal all the physical details of the antenna inside an enclosing sphere, and only to consider the fields outside the sphere. For each TM_{m0} Hankel-Legendre mode he then considered the apparent impedance implied by the ratio of electric and magnetic fields. This is possible for the modes because the ratio of electric (E_θ) and magnetic (H_ϕ) fields is constant at all points on the spherical surface. For example the fundamental mode¹ has the following normal field components:

$$H_\phi = A_1 \cos\theta H_1^1(kr), \quad (1)$$

and

$$E_\theta = A_1 \cos\theta \left[\frac{2}{kr} H_1^1(kr) - H_2^1(kr) \right], \quad (2)$$

which clearly vary in the same way ($\cos\theta$) over the spherical surface. Having the impedance $Z = E_\theta/H_\phi = |Z|e^{i\delta}$ we might treat it as a reactive, X , and resistive, R , series circuit and define the Q as:

$$Q = X/R = \tan\delta. \quad (3)$$

This is a reasonable approximation where one type of energy storage predominates, such as the electric energy in

¹The Author is with the Department of Computer Science and Electrical Engineering, The University of Queensland. Queensland Australia 4072.

¹Chu uses the complete set of modes, which, being orthogonal to each other, can be treated separately.

the case of electric dipoles at small radii. However when the two kinds of energy storage are closer in magnitude, the approach will underestimate Q . A more complex approach is taken by Chu in assuming the impedance represents a series RLC circuit. In this case the Q is given by:

$$Q = \frac{\omega}{R} \left[\frac{dX}{d\omega} - \frac{X}{\omega} \right]. \quad (4)$$

It is worth noting that Chu neglected the frequency dependence of the resistive component of the impedance in his implementation of the above equation.

Let's take a moment to consider what Chu was really doing because the physical principles are somewhat obscured by the use of circuit analogues. Only the fundamental mode for the fields is considered. If we consider the Poynting flux:

$$S = E_\theta H_\phi^* = |S|e^{i\delta}, \quad (5)$$

and we can use (3) as before. Thus we are considering the ratio of real power flux radiated through the sphere to that flowing back and forth between the space outside the sphere and some assumed internal storage of opposite type. Therefore, in using the Q analysis of Chu we assume that an optimal antenna exists inside the sphere which provides just sufficient energy storage inside itself to tune the reactive power storage of the space outside the sphere. The discussion relating to this very abstract notion of possible antenna geometries ranges from Balanis' tautological "(an ideal) antenna utilises efficiently the available volume inside the sphere" [2] to Wheeler's more prescriptive small spherical inductor which is "conceptually filled with perfect magnetic material, so there is no stored energy inside the sphere" [3]. Of course Wheeler's magnetic dipole wound on perfect magnetic material would require a capacitor for matching. A practical electric dipole designed to minimise internal energy storage is that of Goubau [4]. Chu avoided the issue of the distribution of sources inside the sphere, knowing that his complete set of orthogonal modes outside could accommodate any axi-symmetric distribution.

Using the Poynting flux approach, we can integrate over the sphere surface and obtain the total power flow:

$$P = r^2 \int_0^\pi d\theta \int_0^{2\pi} d\phi E_\theta H_\phi^* \sin\theta = |P|e^{i\delta}, \quad (6)$$

and continue to use 3, though now we are liberated from the requirement that the ratio of E to H be constant over the sphere. We can also use the equivalent of (4):

$$Q = \frac{\omega |P|^2}{\Re(P)} \left[\frac{d}{d\omega} \Im\left(\frac{1}{P}\right) - \frac{1}{\omega} \Im\left(\frac{1}{P}\right) \right] \quad (7)$$

where

$$\frac{d}{d\omega} \Im\left(\frac{1}{P}\right) \approx \frac{1}{\Delta} \left[\frac{\Re(1/P(\omega))}{\Re(1/P(\omega + \Delta))} \Im\left(\frac{1}{P(\omega + \Delta)}\right) - \Im\left(\frac{1}{P(\omega)}\right) \right]. \quad (8)$$

In (8) the impedance transformation ratio is varied with frequency to keep the apparent resistance constant, thus better matching the series RLC circuit on which (4) is based.

Clearly, Chu's approach as it stands is impractical when we consider the half-space geometry characteristic of GPR. In this case, his Hankel-Legendre modes fail to satisfy the boundary conditions. Conical Hankel eigenfunctions following the method of Sommerfeld do satisfy the boundary conditions, but unfortunately one or two such eigenfunctions don't describe the fields of even the simplest sources like the point source. In extending the Chu approach to the GPR context, a very substantial, but useful, concession was made: The source was assumed to be a point source at the centre of Chu's sphere. This was encouraged by the observation that the fundamental mode of Chu's approach approximates the fields of a point source in free space. The idea was then to simply integrate the Poynting flux of a point source (VED and HED) over a closed surface containing the theoretical antenna and compute the Q using equation (7).

The next step in the process is also somewhat arbitrary. That is the choice of the surface over which to integrate. Following Chu and using a sphere centred on the source seems artificial in the GPR case. Sources will often be within a few percent of a wavelength of the surface, hence the sphere will need to dip below the surface. The antenna can't possibly occupy the below ground part of the sphere, however, and optimally exclude energy storage from here. The sphere will thus lead to a low estimate of the Q. Alternatively, using a spherical above ground part and a flat disc at the surface creates greater problems in that it greatly overestimates the Q. That is because a real antenna, such as a bowtie, has distributed sources, whereas the point source will create nearly singular fields below the surface in the immediate neighbourhood of the source if the source is close to the ground as suggested above. The spherical surface centred upon the point source was thus chosen as the least problematic of the two methods.

II. METHODS

The fields of the HED and VED are calculated using the Sommerfeld choice vector potentials for the half-space. The spectral form of the dyadic components, G_{xx} , G_{zx} , G_{zz} for the reflected and transmitted components for the half-space are documented in numerous places[5],[6],[7]. For this work, they were integrated numerically. Mixed potentials were not used, but the fields were calculated directly using:

$$\mathbf{E} = \frac{i\omega}{k^2} (\nabla \nabla \cdot + k^2) \mathbf{A} \quad (9)$$

$$\mathbf{H} = \frac{1}{\mu} \nabla \times \mathbf{A} \quad (10)$$

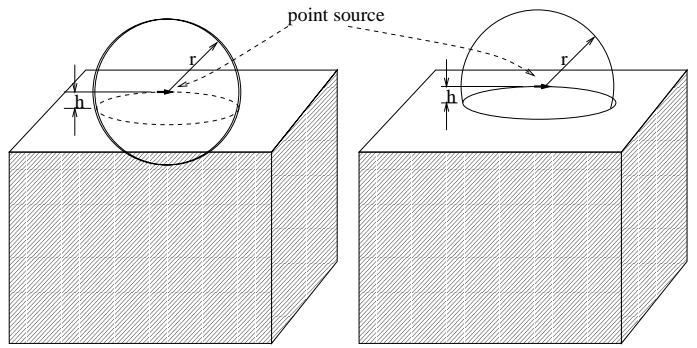


Fig. 1. Alternative surfaces for integration of the Poynting flux: On the left, a sphere which extends below the surface if $r > h$ (This is the actual surface used); On the right, a truncated sphere which extends to the ground surface only, and is closed by the disc area on the ground's surface.

where

$$\mathbf{A} = \hat{x}G_{xx} + \hat{z}G_{zx} \quad (11)$$

for the x-oriented HED, and

$$\mathbf{A} = \hat{z}G_{zz} \quad (12)$$

for the VED.

A. Results

VED and HED sources above a half-space of $\epsilon_r = 9$, $\sigma = 0S/m$ were modelled at 300MHz. The distance parameters in metres r, h can then be considered $r/\lambda, h/\lambda$. The resulting Poynting flux real and imaginary components are shown in figure 2 for the VED and figure 3 for the HED. A check on the convergence of the integrations is given by the constancy of the real component of Poynting flux as a function of sphere radius for these lossless half-spaces. The first difference noticed is the increase in real Poynting flux as the dipoles approach the surface. This is a sensible result. If immersed in the denser half space, a dipole's radiated power increases by $\sqrt{\epsilon_r}$. An interesting result is the change in sign of imaginary Poynting flux component for the larger radius spheres in some cases. In free space, the energy stored external to the sphere always appears (nett) capacitive in the case of electric dipoles. For some cases in the half-space environment, the nett storage external to the sphere changes from capacitive to inductive. Closer inspection of the imaginary Poynting flux at various points on the sphere surface reveals that it is capacitive in some regions (generally above the surface) and inductive in others (generally below the surface). The variation of sign for the imaginary component of Poynting flux is shown in figure 4 for the VED, where the field distributions are symmetric about the vertical axis. The sign variation is perhaps a result of the surface not properly conforming to the natural shape dictated by the electromagnetics. Possible variations on the theme include using a smaller sphere below the surface with conical adaptor section, to follow the equiphas surface.

For most conditions and radii, however, the data based on the sphere provide a useful guide to the likely appli-

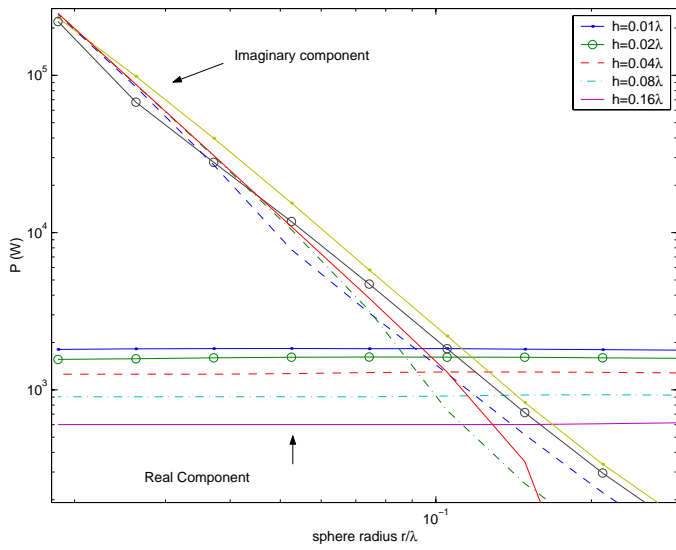


Fig. 2. Total integrated pointing flux for VED above $\epsilon_r = 9, \sigma = 0$ for various sphere radii. The real part is included as a check on the convergence of the integral: It should be constant as shown.

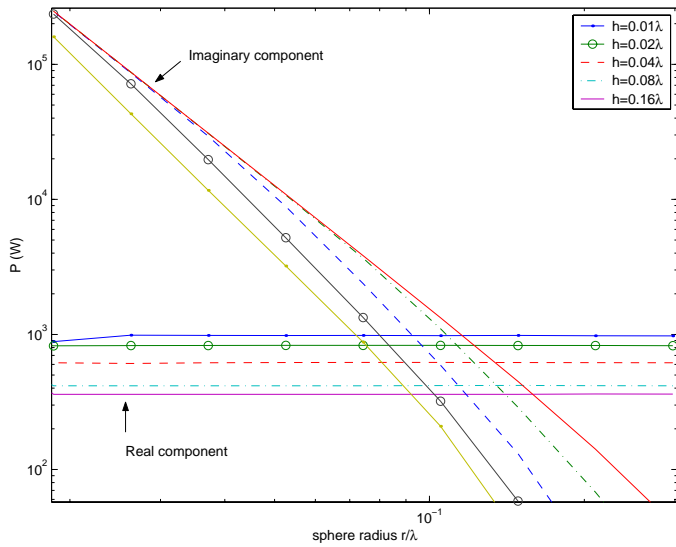


Fig. 3. Total integrated pointing flux for HED above $\epsilon_r = 9, \sigma = 0$ for various sphere radii. The real part is included as a check on the convergence of the integral: It should be constant as shown.

cation of Chu's principle to the small GPR antenna. In figure 5 the result of applying equation (7) to the data for the HED gives the theoretical minimum Q for horizontally polarised GPR antennas above $\epsilon_r = 9, \sigma = 0$ ground. Looking at this plot, we see that similar minimum Q values are achieved in antennas of half the size relative to free space, if the phase centre of the antenna can be brought within 0.01λ of the ground. This is reasonable, as the size reduction would be one third if the antenna was immersed in a homogeneous medium of $\epsilon_r = 9, \sigma = 0$.

In figure 6 the result of applying equation (7) to the data for the VED gives the equivalent result for vertically polarised GPR antennas above $\epsilon_r = 9, \sigma = 0$ ground. The results suggest that the VED is less sensitive to height with similar values of Q for antennas up to 0.08λ such antennas

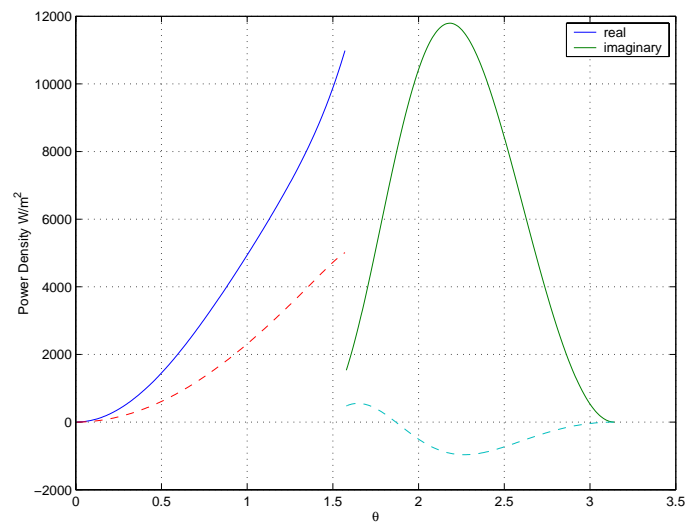


Fig. 4. Poynting flux component normal to the sphere for $h = 0.01\lambda$ and $R = 0.21\lambda$ and $\epsilon_r = 9, \sigma = 0$. Note that above the ground, the stored energy appears capacitive, whereas in places it appears inductive beneath the ground.

being approximately 0.65 the size of free space antennas of the same Q.

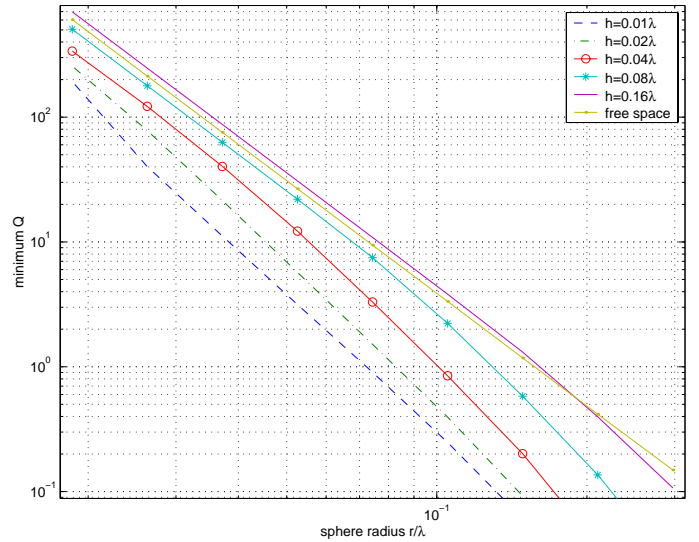


Fig. 5. Theoretical minimum Q of horizontally polarised GPR antennas above a half-space of $\epsilon_r = 9, \sigma = 0$ as a function of containing sphere radius, for various heights of the sphere centre above the surface.

In figures 7 and 8 the minimum Q calculation is applied to a less dense half-space of $\epsilon_r = 4, \sigma = 0$. As would be expected, the effects of the half-space on the minimum Q is less. Equivalent values of Q occur in antennas reduced in size by 0.85 relative to the free-space case.

III. DISCUSSION

In applying this theory to actual antennas, one point to consider is the meaning of the position of the point source. In real antennas the source is spread in one or more dimensions. If we consider resistive Wu-King dipoles, which ap-

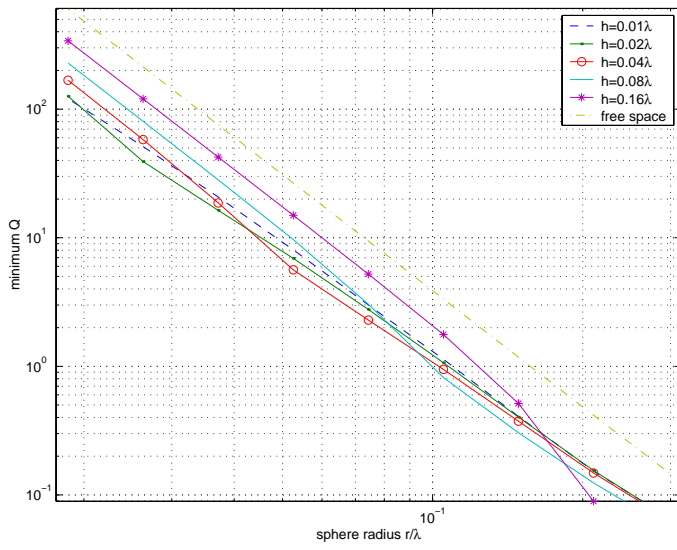


Fig. 6. Theoretical minimum Q of vertically polarised GPR antennas above a half-space of $\epsilon_r = 9, \sigma = 0$ as a function of containing sphere radius, for various heights of the sphere centre above the surface.

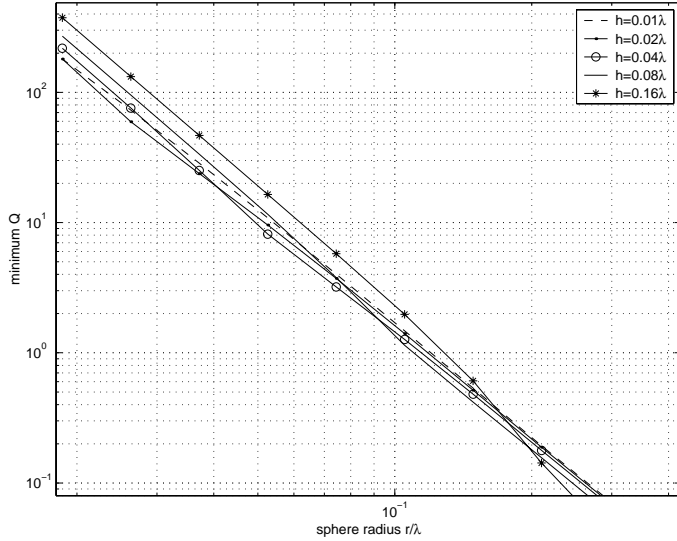


Fig. 7. Theoretical minimum Q of vertically polarised GPR antennas above a half-space of $\epsilon_r = 4, \sigma = 0$ as a function of containing sphere radius, for various heights of the sphere centre above the surface.

pear to be the best method of coupling losses to the stored energy, the strongest source density occurs at the feed point and tapers linearly with distance. The point source modelled is thus a reasonable surrogate for the feed point of the dipole, and we may take the height h as the height of the dipole's axis. The results could also be cautiously applied to the horizontal bowtie, once again using the height of the bowtie as equivalent to the source height.

Returning to the commercial GPR antenna mentioned in the introduction, the length of 2m, centre frequency 35MHz, corresponds to a bounding sphere radius of 0.11λ . Considering figure 5, in free space the minimum Q would be 3, giving an undamped relative bandwidth of 33%, which

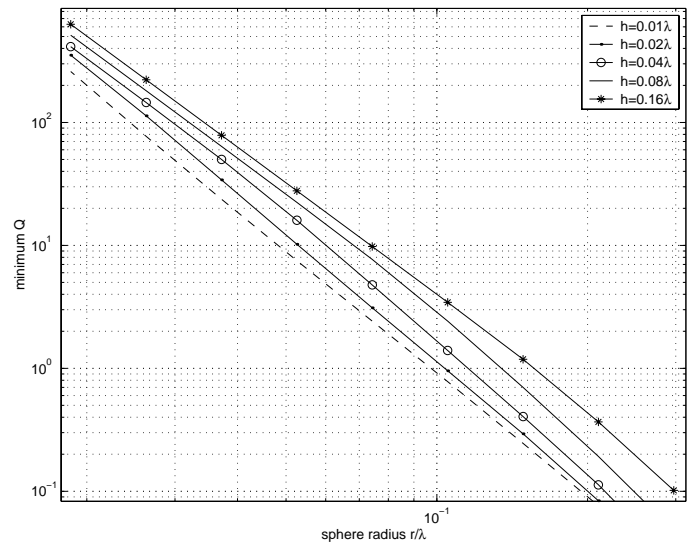


Fig. 8. Theoretical minimum Q of horizontally polarised GPR antennas above a half-space of $\epsilon_r = 4, \sigma = 0$ as a function of containing sphere radius, for various heights of the sphere centre above the surface.

is much less than required. If the antenna were vehicle mounted, a practical height would be 0.2m or 0.023λ . The minimum Q is now 0.5 above $\epsilon_r = 9$ (figure 5) or 1 above $\epsilon_r = 4$ (figure 8). The antenna will thus require minimal additional resistive losses to achieve the required GPR relative bandwidth of 1 as a result of its reduced size. Of course if the antenna were shielded or had additional elements in close proximity to achieve “front to back” ratio then the Q could be well in excess of this minimum.

IV. CONCLUSIONS

A numerical approach was taken in applying Chu's small antenna theory to the case of GPR antennas, which being situated above a dielectric half-space, can't use the Hankel-Legendre spherical basis functions. Although this requires a loss of generality due to the use of a single point source, the results give more certainty to the designer in determining when she is approaching the fundamental limit equivalent to the radian sphere in free space.

For reasonable separations of the phase centre (equivalent to the point source location) of the order 0.08λ , the same minimum Q values occur for smaller antennas. Above a $\epsilon_r = 9$ half space, the reduction in size is 0.65 for HED. For phase centre at 0.16λ , however the antenna Q is very close to that of free space.

In the case of VED, the behaviour is less simple, with higher antennas having smaller Q in the case of larger bounding spheres. The typical value of size reduction is in general less sensitive to height changes and a typical value for the $\epsilon_r = 9$ half-space is also 0.65. As would be expected, the $\epsilon_r = 4$ half-space has size reduction factors closer to unity, of typically 0.85.

The work covered in this paper was part of the ARC SPIRT funded project with Geophysical Technology Limited “Method of Moment Modelling for Improved Detection and Identification of Land Mines and Unexploded Ordnance using Ground Penetrating Radar”. Thanks are also extended to Steve Griffin, Glen Sticklely, Nicholas Shuley, and Dennis Longstaff for their help and advice during the project.

REFERENCES

- [1] L.J.Chu, “Physical limitations of omni-directional antennas”, *Journal of Applied Physics*, vol. 19, pp. 1163–1176, Dec 1948.
- [2] C.A.Balanis, *Antenna Theory Analysis and Design*, John Wiley and Sons, 1982.
- [3] H.A.Wheeler, “Small antennas”, in *Proc. Workshop on Electrically Small Antennas ECOM, Ft. Monmouth N.J.*, May 1976, pp. 17–24.
- [4] G.Goubau, “Multi-element monopole antennas”, in *Proc. Workshop on Electrically Small Antennas ECOM, Ft. Monmouth N.J.*, May 1976, pp. 63–67.
- [5] W.C.Chew, *Waves and Fields in Inhomogeneous Media*, The IEEE Press, 1995.
- [6] C.J.Leat, *Modelling and Design of GPR Antennas*, PhD thesis, University of Queensland, 1999.
- [7] Krzysztof A. Michalski, “The mixed potential electric field integral equation for objects in layered media”, *AEU*, vol. 39, no. 5, pp. 317, 1985.